

Production of intermediate-mass dileptons in relativistic heavy ion collisions

Ioulia Kvasnikova and Charles Gale
*Department of Physics, McGill University,
 3600 University Street, Montréal, QC, H3A 2T8 Canada*

Dinesh Kumar Srivastava*
*Department of Physics, Duke University, Durham, NC 27705
 (October 27, 2018)*

The production of intermediate mass dileptons in ultrarelativistic nuclear collisions at SPS energies is studied. The acceptance and detector resolution inherent to measurements by the NA50 experimental collaboration are accurately modeled. The measured centrality dependence of the intermediate mass lepton pair excess is also addressed.

I. INTRODUCTION

The study of relativistic heavy ion collisions derives its unique importance from the opportunity of producing hot and dense strongly interacting matter. More specifically, one of the hopes is the creation and study of a quark-gluon plasma (QGP), a prediction of QCD [1], which filled the nascent Universe roughly a microsecond after the Big Bang. This field of endeavour currently represents a cutting edge of research in subatomic physics and has generated tremendous activity, both in theory and in experiment [2]. Good penetrating probes of in-medium phenomena in heavy ion collisions are electromagnetic observables, owing to their small rescattering cross sections and to their privileged coupling to vector mesons [3]. For collisions at ultrarelativistic energies, the lepton pair invariant mass (M) spectrum can roughly be divided in three regions: low mass ($M < m_\phi$), high mass ($M > m_{J/\psi}$), and intermediate mass. The high mass region is Drell-Yan-dominated at the CERN SPS, and this contribution is in principle calculable within the realm of perturbative QCD. In connection with the low mass sector in heavy ion collisions at similar energies, the measurements of the CERES collaboration [4] have been seminal in building the case for an observation of in-medium effects on the vector meson spectral densities [5]. There, the experimental collaboration has identified an excess over the sources that were known to be sufficient for the understanding of the spectra in pA collisions. This modification of the vector meson properties in matter represents an exciting discovery and is a genuine consequence of many-body physics.

In the intermediate invariant mass region, an excess of dimuons over the sources expected from pA measurements has also been identified experimentally by the Helios/3 [6] and NA50 [7] collaborations. Some excitement and interest have also been associated with this observation as this mass region is the one originally predicted to contain a plasma signal [8]. Theoretical models have been devised to understand this dimuon excess. Those include rescattering of the open charm mesons with the surrounding hadronic constituents [9]. This approach can not however reproduce the dimuon mass and transverse momentum spectra for central nuclear collisions [10]. An overall charm production enhancement has also been invoked as a prospective interpretation [7]. Whereas this scenario raises an interesting possibility, it has to be reconciled quantitatively with the observation of J/ψ suppression. This issue can however be settled by a direct measurement [11]. An earlier theoretical study of the Helios/3 measurements has attributed the excess to secondary hadronic reaction processes [12]. This result has some consequences that are important to put on a firmer basis, by comparing with other newer data. In this strain, more recent NA50 results have also been interpreted by thermal models, with some quark-gluon content [13,14].

Our goal in this paper is to consider the NA50 intermediate mass dimuon results in the light of a hydrodynamic modeling of the nuclear dynamics, of a detailed analysis of the hadronic dilepton rates, and of a precise simulation of the detector acceptance and resolution. The issue of centrality dependence of the signal is also addressed. The next section briefly describes the hydrodynamic approach utilized, along with its reproduction of hadron spectra. The dilepton rate calculation is then described and the numerical modeling of the detector cuts and resolution is introduced.

*Permanent address: Variable Energy Cyclotron Centre, 1/AF Bidhan Nagar, Kolkata 700 064, India

After the dilepton spectra in invariant mass and transverse momentum have been discussed, the centrality dependence is considered. The paper closes with a summary and a conclusion.

II. HYDRODYNAMIC EVOLUTION AND HADRON SPECTRA

It is well known that the final yield of the thermal dileptons has to be obtained by an integration over the space-time history of evolution of the interacting system. We shall assume that a thermally and chemically equilibrated quark-gluon plasma is produced in such collisions at a time τ_0 , which may be estimated from the condition of isentropic expansion of the plasma [15]:

$$\frac{2\pi^4}{45\zeta(3)} \frac{1}{A_T} \frac{dN}{dy} = 4aT_0^3\tau_0 \quad (2.1)$$

where dN/dy is the particle rapidity density for the collision, and $a = 42.25\pi^2/90$ for a plasma of massless u, d, s quarks, and gluons. The number of flavours is taken to be $N_f \approx 2.5$ to account for the mass of strange quarks. We see that once the transverse area of the colliding system A_T is known, along with dN/dy , the above relation uniquely relates T_0 to τ_0 . While one may get arbitrary large value of T_0 by choosing a smaller formation time of the plasma, the uncertainty principle provides a lower physical limit on $\tau_0 \sim 1/3T_0$ [16].

While considering Pb + Pb collisions at SPS energies, we have taken the average particle rapidity density as 750 for the 10% most central Pb + Pb collisions at the CERN SPS energy, as measured. We estimate the average number of participants for the corresponding range of impact parameters ($0 \leq b \leq 4.5$ fm) as about 380, compared to the maximum of 416 for a head-on collision. We thus use a mass number of 190 to get the radius of the transverse area of the colliding system and neglect its deviations from azimuthal symmetry, for simplicity. As the deviation measured in terms of the number of participants is marginal ($< 9\%$), we expect the error involved also to be small. We also recall that the azimuthal flow is minimal for near central collisions.

The plasma is then assumed to undergo a boost-invariant longitudinal expansion and an azimuthally symmetric radial expansion, with a transition to a hot hadronic gas consisting of *all* hadrons having $M < 2.5$ GeV, in a thermal and chemical equilibrium at a transition temperature T_c . This makes for a rich equation of state. Once all parton matter is converted into hadronic matter, we assume the hot hadronic system to continue to expand until it undergoes a freeze-out at some temperature T_F . During this evolution, the speed of sound of the matter is consistently calculated at every temperature to be used in the equation of state needed for solving the hydrodynamic equations [17].

It is important to realize that the (pressure) gradients in the system cause and control the radial expansion of the plasma, which in turn leads to a more rapid cooling and to the development of a transverse velocity for the fluid. Support for these ideas comes from intensity interferometry and from measured particle spectra. It is thereby necessary to have a proper initial energy density profile as it affects the hydrodynamic developments by introducing additional gradients. We assume it to follow the so-called “wounded-nucleon” distribution, which for central collision of identical nuclei leads to:

$$\epsilon(\tau_0, r) \propto \int_{-\infty}^{\infty} \rho(\sqrt{r^2 + z^2}) dz \quad (2.2)$$

where ρ is the (Woods-Saxon) distribution of nucleons and r is the transverse distance. This is prompted by the experimental observation that transverse energy deposited in these collisions scales with the number of participants. The normalization is then determined through numerical integration such that

$$A_T \epsilon_0 = \int 2\pi r \epsilon(r) dr. \quad (2.3)$$

A proper profile is also needed to get a quantitative description of the dilepton yields and through this to infer the initial conditions. It is clear that the energy densities at larger r would be smaller, implying lower temperatures and a shorter life-time till the fluid there undergoes freeze-out. Now recall that the four-volume $d^4x = \tau d\tau r dr d\eta d\phi$ and thus the contribution of a given fluid element rises linearly with its transverse distance, which further “magnifies” the contribution from large r . One can immediately see that a uniform energy density profile often employed in the literature would lead to an erroneously large contribution from large r . This fact plays an important role in arriving at the required initial conditions.

We now have all the ingredients to solve the hydrodynamic equations. This is done through the procedures described in Refs. [17,18].

A. Initial conditions at the SPS

On the basis of the rapidity density etc. observed at SPS energies in central collisions involving lead nuclei, it was shown recently [19] that a good empirical description of the single photon data measured by the WA98 collaboration was obtained when the plasma formation time was taken to be $\tau_0 = 0.2$ fm/c. This corresponded to an average initial temperature of about 330 MeV. In the present work, we shall use these values but also explore the consequences of varying τ_0 and T_0 , keeping the resulting dN/dy fixed.

The phase transition is assumed to take place at $T = 180$ MeV and the freeze-out at 120 MeV. This value of the critical temperature is motivated by lattice QCD results which give values of about 170 – 190 MeV [1], and the thermal model analyses of hadronic ratios which suggest that the chemical freeze-out in such collisions takes place at about 170 MeV (recent analyses yield a value of 158.1 ± 3.2 MeV [20] for the chemical freeze-out temperature). The phase transition should necessarily take place at a higher temperature.

B. Hadronic Spectra

As a first step we look at the spectra of several hadrons for the central collision of lead nuclei measured at the SPS.

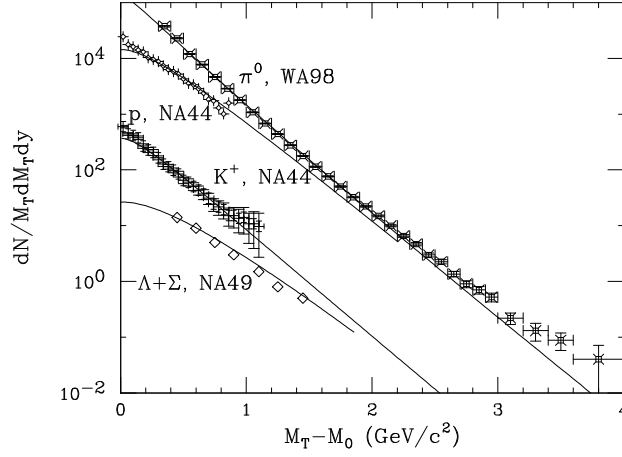


FIG. 1. Hadronic spectra in central collision of lead nuclei at SPS energy. The formation time is assumed to be 0.2 fm/c. The data are for pions, protons, kaons, and lambdas + sigmas, from top to bottom, respectively.

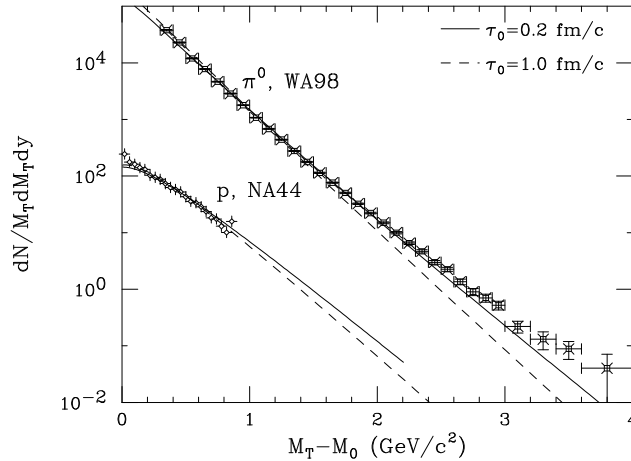


FIG. 2. Hadronic spectra in central collision of lead nuclei at SPS energy. The formation time is taken as 0.2 fm/c and 1 fm/c respectively.

In Fig. 1 we show our results when the formation time is taken as $\tau_0 = 0.2 \text{ fm}/c$ as in Ref. [19]. The data are from Refs. [21–23]. Even though it is known for quite some time that a reasonable variation of the initial temperature and the formation time, keeping the corresponding dN/dy fixed, affects the flow only marginally, we study the consequences of increasing τ_0 to $1 \text{ fm}/c$ in Fig. 2. We see that the hadronic spectra shapes are relatively insensitive to such variations in the initial conditions, as the flow takes some time to develop. In all cases, the agreement is quite good. This fact lends some credibility to the dynamics advocated here.

III. DILEPTON SPECTRA AT SPS ENERGY

A. Dilepton emission rates

For the dilepton emission from the deconfined sector of QCD, we have assumed that the dominating process is $q\bar{q} \rightarrow \ell^+\ell^-$. The emission rates that correspond to this process have been calculated many times. An example of their quantitative contribution can be found in Ref. [24]. Even though those rates are the Born terms in the parton sector, a very recent lattice calculation has found that those were surprisingly accurate [25].

In the evaluation of hadronic rates most calculations have relied on effective Lagrangian techniques, where the available parameters are fitted to empirical measurements. An example of the application of this line of thought to the low mass dilepton sector can be found in Refs. [5,26]. A problem which arises when one tries to extend those techniques to the intermediate mass region is the appearance of off-shell effects. Indeed, different approaches that agree in the soft sector can yield widely different results in higher invariant mass extrapolations [27]. Fortunately, constraints on the hadronic processes can be obtained through the wealth of data of the type $e^+e^- \rightarrow \text{hadrons}$ [28]. In addition, those measurements cover exactly the same invariant mass range as the one which concerns this work. Those have been used, together with τ -decay data, to construct the vector and axial-vector spectral densities [29]. Similarly, the intermediate invariant mass initial state e^+e^- data has been analyzed specifically in the most important exclusive channels. This information can then be used to construct rates for hadrons $\rightarrow e^+e^-$ [12]. It is this procedure that is followed in the current work. The contributing channels producing lepton pairs in the invariant mass range $1 \text{ GeV} < M < 3 \text{ GeV}$ have been found to correspond to the initial states: $\pi\pi$, $\pi\rho$, $\pi\omega$, $\eta\rho$, $\rho\rho$, πa_1 , $K\bar{K}$, $K\bar{K}^* + c.c.$ [12,30]. A detailed channel-by-channel discussion is too long to be had here, but a quantitative assessment of the net dilepton rate from a gas of mesons at $T = 150 \text{ MeV}$ is shown in Fig. 3. Also shown is the rate extracted from the spectral function evaluation [29,31]. In principle, the latter contains all the hadronic sources. The correspondence between those two results is a confirmation that the important channels have indeed been identified in the hadronic scenario.

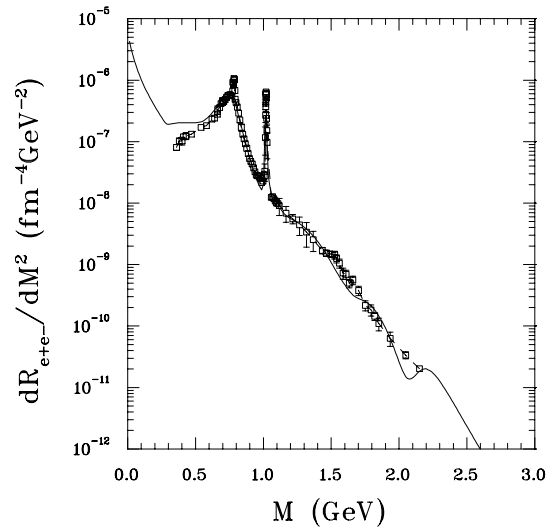


FIG. 3. Net dilepton production rate from a gas of mesons at a temperature of $T = 150 \text{ MeV}$, as a function of dilepton invariant mass. The full curve is the sum of the hadronic channels discussed in the text and in the references. The data points follow from an extraction of spectral densities from e^+e^- scattering experiments [29,31].

Using the rates of dilepton production from quark and hadronic matter, it is straightforward to calculate the spectra for dileptons, say for the central collision of lead nuclei at SPS energy. We add the contributions of the quark matter from the QGP phase and the quark matter part of the mixed phase and call it QM. Similarly we add the contributions of the hadronic matter part of the mixed phase and the hadronic phase and call it HM. The contribution of the Drell-Yan process is obtained by a scaling of nucleon-nucleon estimates to the case of nucleus-nucleus collisions. We get the results shown in Fig. 4, no acceptance or resolution corrections are implemented. It is clear that in principle, if the formation time is small (*i.e.*, the initial temperature is large) then there could be a substantial contribution of the dileptons having their origin in the quark matter, in the intermediate mass window. Note that the HM contribution is only very marginally affected by variations in the τ_0 . We shall proceed to model the effect of detector resolution and to compare with experimental measurements.

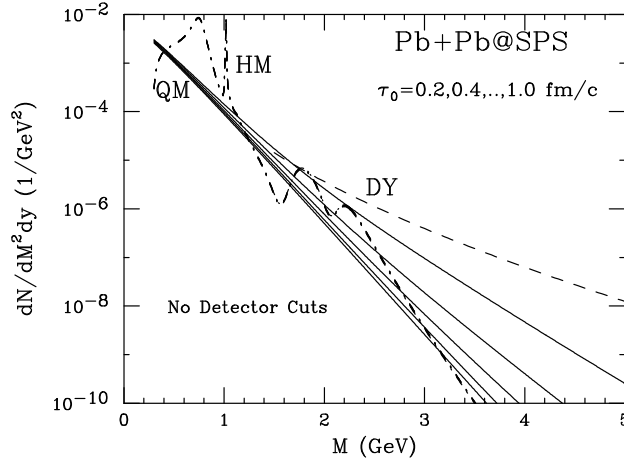


FIG. 4. The net yield of lepton pairs from the quark gluon plasma, Drell-Yan and the hadronic sources are shown separately, before detector and acceptance corrections. The QGP signal for different formation times τ_0 are shown (solid lines), earlier time on top, later times on the bottom. The Drell-Yan contribution is the dashed line, and the hadronic matter contribution the dashed-dotted curve. The yield from correlated open charm decay is not shown here. That source's contribution to dN/dM is a decaying exponential in the mass range under scrutiny and its dependence on various parameter assumptions is discussed in detail in [10].

B. Detector acceptance and dilepton spectra

It is vital to account for the finite acceptance of the detectors and for their resolution when comparing the results of theoretical calculations with measured experimental data. Those effects are important in the NA50 experiment [10]. One approach to this problem is to model approximately and analytically the acceptance. While this can be readily implemented [13,32], a legitimate doubt can subsist about the accuracy of the experimental representation, especially in regions where edge effects might be important. In order to circumvent this problem we use here for the first time a numerical subroutine developed to reproduce the NA50 acceptance cuts and finite resolution effects in the measurements of dimuon pairs in Pb + Pb collisions at the CERN SPS [33].

We compute the invariant mass distribution of the dileptons in our hydrodynamic approach and then we run our pairs through the numerical detector simulation. The normalization is determined by a fit to the Drell-Yan data using the MRSA parton distribution functions as in the NA50 analysis. For getting the p_T distribution we supplement our dN/dM^2 estimates for the Drell-Yan with a gaussian distribution in p_T as in Ref. [13] which very closely reproduced the estimates obtained by the NA50 collaboration. The result is shown in Fig. 5. We also compute the p_T distribution for the muon pairs, in the invariant mass window $1.5 < M < 2.5$ GeV. This spectrum is broken down in the same sources as previously and is shown in Fig. 6.

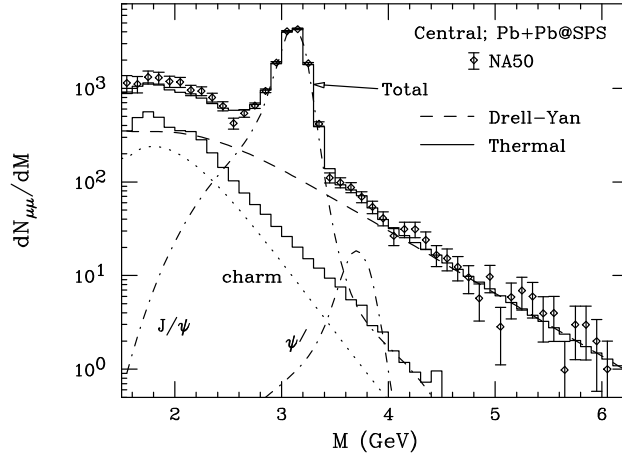


FIG. 5. We show the calculated dimuon invariant mass spectrum after correcting for detector acceptance and resolution. The data is from the NA50 collaboration [7]. The Drell-Yan and thermal contributions are shown separately, as well as those coming from correlated charm decay and direct decays of the J/ψ and ψ' .

At this point it is appropriate to consider the following question: which initial temperature is demanded by the intermediate mass dilepton data? A critical and quantitative assessment of this issue can be obtained by examining a linear plot of the lepton pair spectrum in the mass region under scrutiny. This is shown in Fig. 7. From this figure, it appears that the best fit is provided by $\tau_0 = 0.2$ fm/c, and that the second best (less than two standard deviations away for most of the data points) belongs to $\tau_0 = 0.4$ fm/c. In terms of initial temperature those two values of the formation time correspond to $T_0 \approx 330$ and 265 MeV respectively. A conservative and reasonable point of view is that it is probably not fair in such a challenging and complex environment as that of ultrarelativistic heavy ion collisions to ask for an agreement that is better than two standard deviations, considering the inherent uncertainties. This circumvents the issue of initial temperature determination. Also, there are questions that have to do with the specific dynamics used here to model the nuclear collisions. However in this respect, the hydrodynamic model used in this work is solved self-consistently and its parameters are constrained by the hadronic data as well. In connection with the important discussion on plasma signals the quark matter contribution is $\approx 23\%$ for $\tau_0 = 0.2$ fm/c, and $\approx 19\%$ for $\tau_0 = 0.4$ fm/c, around the lepton pair invariant mass of 1.5 GeV.

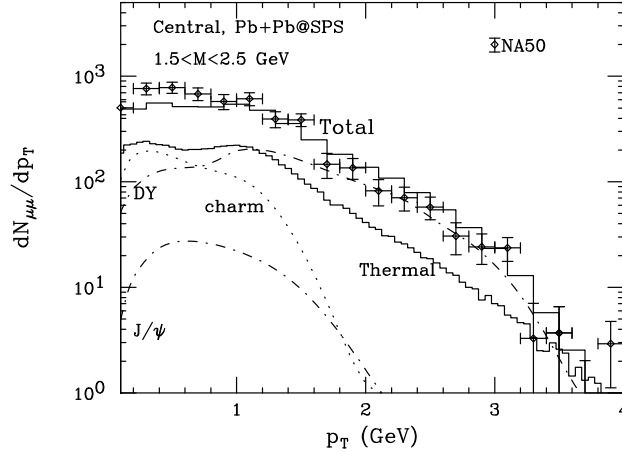


FIG. 6. We show the dimuon transverse momentum spectrum after accounting for detector effects. The origin of the data and of the different sources are as in Fig. 5.

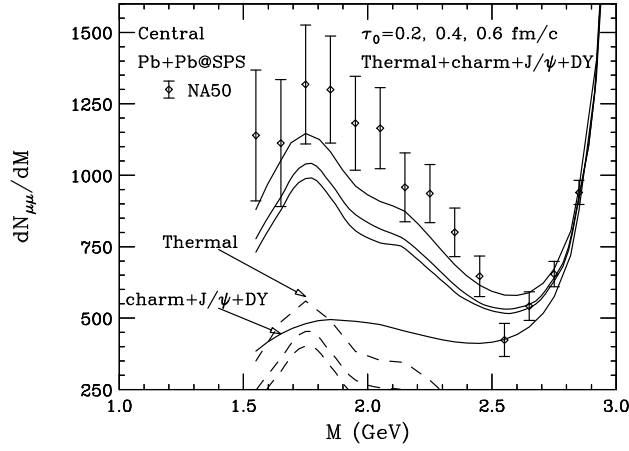


FIG. 7. A linear plot of the net dilepton spectrum in the intermediate mass region. The three solid curves correspond to formation times $\tau_0 = 0.2, 0.4, 0.6$ fm/c, from top to bottom, respectively. The data are from [7]. The thermal contributions and the contribution from hard processes are shown separately.

C. Centrality dependence

Our discussion so far was concerned only with the high multiplicity bin or, with mostly central collisions. To extend the hydrodynamic model to non-central events and to properly treat the azimuthal anisotropy is not a simple task. However, one can get a fair estimate of the centrality dependence by ignoring the broken azimuthal symmetry and by approximating the region of nuclear overlap by a circle of radius $R \approx 1.2(N_{\text{part}}/2)^{1/3}$, where N_{part} is the number of participants [34]. Assuming the uncertainty relationship, $\tau_0 = 1/3T_0$, one can track the changing multiplicities without introducing additional parameters. The results of this exercise are shown in Fig. 8, for S + U and Pb + Pb collisions. Also shown are the contributions from the “enhanced production of charm” estimated by the NA50 collaboration, normalized to the dileptons estimated by us. We estimate the contribution of the “excess charm” ΔN_{ch} from

$$\Delta N_{ch} \propto (E - 1)N_{coll} \quad (3.1)$$

where N_{coll} is the average number of collisions for the given centrality and E is the ‘enhancement’ factor given by the NA50 measurement [10]. The constant of proportionality is identical for all the bins for a given system. It is seen that the agreement with the measured data is quite good, and our approach gives a fair description of the centrality dependence of the excess dilepton measurement.

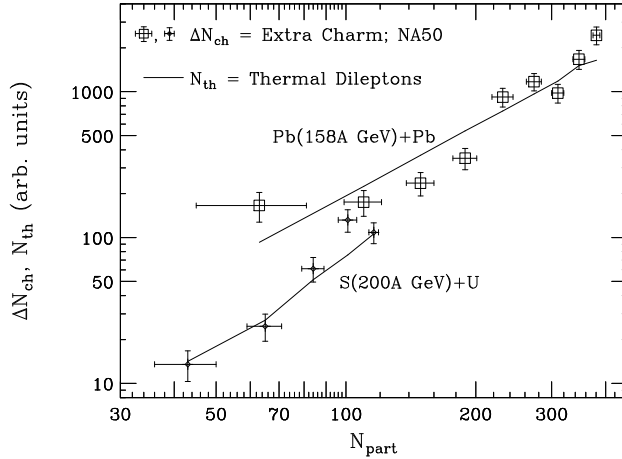


FIG. 8. Centrality dependence. The data represent the “extra charm” yield (as categorized by the NA50 collaboration [7]) needed to describe the intermediate mass region dimuon data. The full curve is from our thermal sources.

IV. SUMMARY AND CONCLUSION

In the light of the findings reported on in this work, it does appear that the case of attributing the intermediate mass dilepton excess to an enhanced charm production rests on evidence that is no longer very compelling. The lepton pairs coming from a thermal hadronic medium comprise an important part of the signal, in agreement with earlier analyses of the Helios/3 measurements [12], and with those of more recent studies [13,14]. It is satisfying to notice that the behaviour of the centrality dependence is also reproduced by the modeling and the dynamics used here. We have also considered the constraints on the initial temperature set by the data in the framework of our approach. There is a QGP component in the treatment used in this work. Unfortunately, its numerical value is not important enough to provide irrefutable evidence. The future of this field is bright: RHIC electromagnetic measurements should soon signal bold incursions into a new territory.

ACKNOWLEDGMENTS

It is a pleasure to acknowledge useful conversations with L. Capelli, O. Drapier, and L. Kluberg. This work was supported in part by the Natural Sciences and Engineering Research Council of Canada, in part by FCAR of the Quebec government, and in part by the US Department of Energy under grant DE-FG02-96ER40945..

-
- [1] F. Karsch, *17th International Symposium on Lattice Field Theory* (Lattice '99), Pisa, Italy, hep-lat/9909006.
 - [2] See, for example, *Proceedings of the 15th. International Conference on Ultrarelativistic Nucleus-Nucleus Collisions (Quark Matter 2001)*, Nucl. Phys. **A** in press, and references therein.
 - [3] J. J. Sakurai, *Currents and Mesons*, (University of Chicago Press, Chicago 1969); H. B. O'Connell, B. C. Pearce, A. W. Thomas, and A. G. Williams, Prog. Part. Nucl. Phys. **39**, 201 (1997).
 - [4] H. Appelshaeuser, *Proceedings of the 15th. International Conference on Ultrarelativistic Nucleus-Nucleus Collisions (Quark Matter 2001)*, Nucl. Phys. **A** in press, and references therein.
 - [5] R. Rapp and J. Wambach, Adv. Nucl. Phys. **25**, 1 (2000).
 - [6] M. Masera *et al.*, Nucl. Phys. **A590**, 93c (1995); A. L. S. Angelis *et al.*, Eur. J. Phys. C **13**, 433 (2000).
 - [7] M. C. Abreu *et al.*, NA50 Coll. Eur. Phys. J. C **14**, 443 (2000).
 - [8] E. V. Shuryak, Phys. Lett. **78**, 150 (1978).
 - [9] Z. Lin and X. N. Wang, Phys. Lett. **B444**, 245 (1998).
 - [10] L. Capelli, Ph. D. thesis, Université Claude Bernard (2001).
 - [11] <http://na61.web.cern.ch/NA61/>
 - [12] G. Q. Li and C. Gale, Phys. Rev. Lett. **81**, 1572 (1998); Phys. Rev. C **58**, 2914 (1998).
 - [13] R. Rapp and E. Shuryak, Phys. Lett. **B473**, 13 (2000).
 - [14] K. Gallmeister *et al.*, Nucl. Phys. **A688**, 939 (2001).
 - [15] J. D. Bjorken, Phys. Rev. D **27**, 140 (1983); R. C.Hwa and K. Kajantie, Phys. Rev. D **32**, 1109 (1985).
 - [16] J. Kapusta, L. McLerran, and D. K. Srivastava, Phys. Lett. B **283**, 145 (1992).
 - [17] J. Cleymans, K. Redlich, D.K. Srivastava, Phys. Rev. C **55**, 1431 (1997); J. Cleymans, K. Redlich, D. K. Srivastava; Phys. Lett. B **420**, 261 (1998).
 - [18] H. von Gersdorff, L. McLerran, M. Kataja, and P. V. Ruuskanen, Phys. Rev. D **34**, 794 (1986); P. V. Ruuskanen, Acta Phys. Pol. B **18**, 551 (1986).
 - [19] D. K. Srivastava and B. Sinha, Phys. Rev. C **64**, 034902 (2001).
 - [20] See, e.g., P. Braun-Munzinger, I. Heppe, and J. Stachel, Phys. Lett. B **465**, 15 (1999) See, e.g., P. Braun-Munzinger, I. Heppe, and J. Stachel, Phys. Lett. B **465**, 15 (1999); F. Becattini, J. Cleymans, A. Keranen, E. Suhonen, and K. Redlich, Phys. Rev. C **64**, 024901 (2001).
 - [21] M. M. Aggarwal *et al.*, Phys. Rev. Lett. **81**, 4087 (1998).
 - [22] I. G. Bearden *et al.*, Phys. Rev. Lett. **78**, 2080 (1997).
 - [23] P. G. Jones *et al.*, Nucl. Phys. **A610**, 175c (1996).
 - [24] K. Kajantie, J. Kapusta, L. McLerran, and A. Mekjian, Phys. Rev. D **34**, 2746 (1986).
 - [25] F. Karsch *et al.*, hep-lat/0110208.
 - [26] Ralf Rapp and Charles Gale, Phys. Rev. C **60**, 024903 (1999).
 - [27] Song Gao and Charles Gale, Phys. Rev. C **57**, 254 (1998).

- [28] See, for example, S. I Dolinsky *et al.*, Phys. Rep. **202**, 99 (1991), and references therein.
- [29] Z. Huang, Phys. Lett. **B361**, 131 (1995).
- [30] I. Kvasnikova, Ph. D. thesis, McGill University (2001).
- [31] Z. Huang, private communication.
- [32] Dinesh Kumar Srivastava, Bikash Sinha, Ioulia Kvasnikova, and Charles Gale, *Proceedings of the 15th. International Conference on Ultrarelativistic Nucleus-Nucleus Collisions (Quark Matter 2001)*, Nucl. Phys. **A** in press.
- [33] O. Drapier, for the NA50 collaboration, private communication; NA38 collaboration, Nucl. Instrum. Methods, **A405**, 139 (1998).
- [34] D. K. Srivastava, Phys. Rev. C **64**, 064901 (2001); J.-Y. Ollitrault, Phys. Lett. B **273**, 31 (1991).